JOURNAL OF Evolutionary Biology

doi: 10.1111/jeb.12626

SHORT COMMUNICATION

Dendritic connectivity shapes spatial patterns of genetic diversity: a simulation-based study

I. PAZ-VINAS*†‡ & S. BLANCHET*§

*UMR 5174 EDB (Laboratoire Évolution & Diversité Biologique), Centre National de la Recherche Scientifique (CNRS), École Nationale de Formation Agronomique (ENFA), Université Paul Sabatier, Toulouse, France
†UMR 5174 (EDB), Université de Toulouse, UPS, Toulouse, France
‡Aix-Marseille Université, CNRS, IRD, Université d'Avignon, UMR 7263 – IMBE, Équipe EGE, Centre Saint-Charles, Case 36, Marseille, France
§Centre National de la Recherche Scientifique (CNRS), Station d'Écologie Expérimentale du CNRS à Moulis, USR 2936, Moulis, France

Keywords:

coalescent-based simulations;
dendritic ecological networks;
genetic diversity;
population differentiation;
spatial patterns of biodiversity.

Abstract

Landscape features notoriously affect spatial patterns of biodiversity. For instance, in dendritic ecological networks (such as river basins), dendritic connectivity has been proposed to create unique spatial patterns of biodiversity. Here, we compared genetic datasets simulated under a lattice-like, a dendritic and a circular landscape to test the influence of dendritic connectivity on neutral genetic diversity. The circular landscape had a level of connectivity similar to that of the dendritic landscape, so as to isolate the influence of dendricity on genetic diversity. We found that genetic diversity and differentiation varied strikingly among the three landscapes. For instance, the dendritic landscape generated higher total number of alleles and higher global F_{st} than the lattice-like landscape, and these indices also varied between the dendritic and the circular landscapes, suggesting an effect of dendricity. Furthermore, in the dendritic landscape, allelic richness was higher in highly connected demes (e.g. confluences in rivers) than in low-connected demes (e.g. upstream and downstream populations), which was not the case in the circular landscape, hence confirming the major role of dendricity. This led to bell-shaped distributions of allelic richness along an upstream–downstream gradient. Conversely, genetic differentiation (F_{st}) was lower in highly than in low-connected demes (which was not observed in circular landscape), and significant patterns of isolation by distance (IBD) were also observed in the dendritic landscape. We conclude that in dendritic networks, the combined influence of dendricity and connectivity generates unique spatial patterns of neutral genetic diversity, which has implications for population geneticists and conservationists.

Introduction

Describing patterns of biodiversity (i.e. repetitions of definite biodiversity distributions along geographical or environmental gradients; Lawton, 1996) and shedding light on the foremost processes driving biodiversity patterns are a key concern in ecological and evolutionary sciences (Gotelli *et al.*, 2009; Chave, 2013). Understanding how biodiversity is distributed in space and time indeed improves our predictive capacities, for instance by facilitating the forecasting of the distribution of biodiversity in changing environments (Guisan & Thuiller, 2005). In ecosystems that are strongly structured by complex spatial arrangements, spatial patterns of biodiversity can be influenced by particular landscape features such as topological or environmental constraints (Manel & Holderegger, 2013), and at multiple organizational levels (e.g. genes, species or functional groups;

Correspondence: Ivan Paz-Vinas, Institut Méditerranéen de Biodiversité et d'Écologie (IMBE), UMR 7263 (CNRS – AMU – IRD – Université d'Avignon), 3 place Victor Hugo, Centre Saint-Charles, Case 36, 13331 Marseille Cedex 3, France. Tel.: (+33) 4 13 55 11 57; fax: (+33) 4 13 55 07 86; e-mail: ivanpaz23@gmail.com

Chave, 2013). This is the case for dendritic ecological networks, such as river basins, hedgerows and caves, a type of ecosystem characterized by a hierarchical spatial structure that mimics the branching pattern of trees (Campbell Grant *et al.*, 2007; Altermatt, 2013; Peterson *et al.*, 2013).

Theoretical studies have explored how landscape organization influences spatial patterns of interspecific (Muneepeerakul *et al.*, 2008; Carrara *et al.*, 2012; Seymour & Altermatt, 2014) and intraspecific diversity (Labonne *et al.*, 2008; Chaput-Bardy *et al.*, 2009; Morrissey & de Kerckhove, 2009) in dendritic ecological networks. For instance, Carrara *et al.* (2012) demonstrated that connectivity (i.e. the type and the degree of connection between ecosystem portions) in dendritic ecological networks shapes taxonomic diversity at the meta-community level, by comparing patterns of species diversity between two contrasting landscapes (i.e. a dendritic vs. a lattice-like landscape). At the intraspecific (or meta-population) level, previous theoretical studies focused on the effects of asymmetric gene flow and overland dispersal on spatial patterns of neutral genetic diversity (Chaput-Bardy *et al.*, 2009; Morrissey & de Kerckhove, 2009), and on the effect of the network structure on population demogenetics (Labonne *et al.*, 2008). The latter study specifically showed that dendritic connectivity may influence genetic diversity and differentiation at the meta-population level depending on the degree of ongoing dispersal between patches (i.e. low or high dispersal; Labonne *et al.*, 2008). Although such study suggests that connectivity can influence the spatial distribution of neutral genetic diversity in dendritic ecological networks, we are not aware of any study testing specifically whether or not dendritic connectivity drives spatial patterns of genetic diversity in dendritic ecological networks.

The general objective of this study was to theoretically test whether or not dendritic connectivity shapes spatial patterns of neutral genetic diversity at the meta-population level. Using simulated microsatellite genetic datasets, we first tested the null hypothesis that genetic diversity indices measured at the landscape scale did not vary between meta-populations living in a dendritic landscape and those living (i) in a classical two-dimensional stepping-stone landscape ('lattice landscape') displaying high levels of connectivity among demes and (ii) in a quasi-circular landscape ('circular landscape') characterized by connectivity levels similar to those of the dendritic landscape, but that was not dendritic. Given that increasing connectivity decreases isolation between demes in meta-populations, we expect to reject this null hypothesis for the comparison between the dendritic vs. the lattice landscape, but not for the comparison between the dendritic vs. the circular landscape. We rather predict that within-deme diversity should be higher in the lattice (highly connected) landscape than in the dendritic landscape, whereas the reverse is expected for among-deme genetic differentiation. Concerning the dendritic vs. the circular landscape comparison, rejecting the null hypothesis would imply that differences in genetic diversity and differentiation between the two landscapes arise from structural differences (i.e. dendricity) and not only from the level of connectivity. Second, we tested the working hypothesis that dendritic connectivity generates a nonrandom spatial distribution of genetic diversity in dendritic networks, by (i) characterizing spatial patterns of genetic diversity in the dendritic landscape and by (ii) comparing levels of genetic diversity and genetic differentiation between low vs. highly connected demes in this landscape. It has been empirically shown that genetic differentiation tends to be higher in upstream demes (low connected) than in confluence demes (highly connected) in river networks (Finn *et al.*, 2011; Pauls *et al.*, 2014); this is a pattern we predict to observe for data simulated under the dendritic landscape, but not for those simulated under the circular landscape, which would suggest a strong role of dendricity. Furthermore, we predict that – in the dendritic but not the circular landscape – the most connected demes should harbour the highest within-deme genetic diversities, which may explain yet unresolved patterns observed in the field characterized by higher within-deme genetic diversity at the core of the network (e.g. Watanabe *et al.*, 2008; Alp *et al.*, 2012). Our results, combined with those from other authors (Finn *et al.*, 2011; Carrara *et al.*, 2012; Múrria *et al.*, 2013), constitute a new step towards the understanding of how dendritic connectivity *per se* can shape biodiversity in dendritic ecosystems.

Materials and methods

Simulated genetic data

We used a home-made computational pipeline that allowed handling, generating and analysing multiple simulated genetic datasets under different population genetics models. Specifically, we used the program ABCsampler (Wegmann *et al.*, 2010) to (i) choose model parameter values from prior distributions (defined below) and (ii) feed the coalescent-based genetic data simulator SIMCOAL 2 (Laval & Excoffier, 2004) with these parameter values. We then used the programs ADZE v1.0 (Szpiech *et al.*, 2008) and arlsumstat (Excoffier & Lischer, 2010) to calculate, for each simulated dataset, a set of basic statistics describing genetic diversity at the deme or the whole landscape level (see below). The program PGDSPIDER v2.0 (Lischer & Excoffier, 2011) was also integrated in the pipeline to convert the output files of Simcoal 2 to the input format required by ADZE, and the R statistical software v3.0.1 was used to analyse the data.

This pipeline was used to simulate microsatellite genetic datasets (i.e. 15 independent loci considering

the stepwise mutation model (SMM) and a unique mutation rate $\mu = 5 \times 10^{-4}$) under three contrasting landscapes: (i) a lattice-like landscape (the 'lattice model', Fig. 1a), composed of 36 demes connected in a two-dimensional stepping-stone fashion (Kimura & Weiss, 1964; Fig. 1a); (ii) a quasi-circular landscape (the 'circular model', Fig. 1b), characterized by a circular stepping-stone chain of 27 demes, to which nine single external demes are attached; and (iii) a dendritic network landscape (the 'dendritic model') composed of 29 demes connected in a dendritic fashion, to which a seven-deme-long linear stepping-stone chain is attached (Fig. 1c). Although different in terms of spatial structure, the dendritic and circular models display similar levels of connectivity when considering a simple measure of connectivity (i.e. the number of connections between a deme and its nearest neighbours, see Fig. 1b,c). Accordingly, 'low' connected demes for both models are those being connected to a single other deme (hereafter, C1 demes; Fig. 1b,c), whereas 'highly' connected demes are those being connected to three other demes (hereafter, C3 demes; Fig. 1b,c). In the dendritic model, C1 demes are equivalent to the most upstream and downstream populations of a putative river network, whereas C3 demes correspond to populations situated in confluences. The seven-deme-long linear stepping-stone chain situated in the downstream part of the dendritic model corresponds to the main stem (i.e. the trunk) of a putative river network.

For each model, each deme was characterized by an identical effective population size (hereafter, effective deme size N_e) and a symmetrical pairwise migration rate (MR) with its immediate neighbour(s). We tested the effects of different N_e and MR on genetic diversity by running a total of 35 000 simulations per model, considering three alternative effective deme sizes, corresponding to low (i.e. 10), medium (100) and high (1000) N_e values, and for MR values ranging from 0.01 to 0.5 (proportion of migrants per generation).

We assumed for each model the same combinations of N_e and MR values, so as to allow direct comparisons between dendritic, lattice and circular models. We simulated microsatellite markers because of its wide use in empirical surveys describing patterns of genetic diversity (Putman & Carbone, 2014). Simulations were performed on an ALTIX ICE 8200 EX cluster (Silicon Graphics International, Fremont, CA, USA) hosted by the CALMIP group (University Paul Sabatier, Toulouse, France).

Summary statistics

At the landscape scale, we calculated the total number of alleles, the per deme allelic richness averaged across all demes and over all loci (mean allelic richness), the variance in allelic richness across all demes and the global F_{st} observed over the whole landscape (totNA, meanAR, varAR and global F_{st}, respectively) for each simulation from the lattice, circular and dendritic models. Statistics derived from allelic richness are analogous to measures of α-diversity; totNA is analogous to γ-diversity, whereas statistics derived from the F_{st} index can be seen as measures of β-diversity.

At the deme level and for the dendritic and circular models only, we estimated for each simulation the mean allelic richness over all loci per deme (AR), pairwise genetic differentiation estimates between demes (pairwise F_{st}) and mean pairwise F_{st} values per deme (mean F_{st}; i.e. the mean F_{st} value calculated for each deme from each pairwise comparison with other demes).

Comparison between lattice, circular and dendritic landscapes

We tested whether or not dendritic connectivity influenced α-, β- and γ-diversity in the dendritic landscape by comparing, for each combination of N_e per deme and MR, totNA, mean AR, varAR and global F_{st} values estimated for the dendritic model with those estimated for the lattice and circular models. As an alternative, we also compared (for each model) the relationships between totNA, mean AR, varAR, global F_{st} and the $N_e \times$ MR product. This later parameter is commonly used in theoretical population genetics to quantify the amount of ongoing gene flow between pairs of populations (here, the number of genes that are transferred between pairs of demes each generation).

Comparison between low and highly connected demes in dendritic and circular landscapes

We tested for each simulation generated under dendritic and circular models whether or not AR and mean F_{st} calculated at the deme level varied between low (C1) and highly (C3) connected demes. Specifically, we calculated (for each model and each combination of N_e per deme and MR) differences (in percentage) of AR and mean F_{st} values between C3 and C1 demes (C3–C1). Additionally, we expressed these differences as a function of the $N_e \times$ MR product.

Spatial patterns of genetic diversity in the dendritic landscape

We characterized for each simulation of the dendritic model spatial patterns of genetic diversity, by representing, for each combination of N_e per deme and MR, the relationship between AR and the distance of each deme from the putative river mouth (i.e. the most downstream part of the network, see Fig. 1c), given that an increase in AR in downstream sections is generally assumed in this type of landscape (Pollux *et al.*, 2009; Paz-Vinas *et al.*, 2013). Finally, we

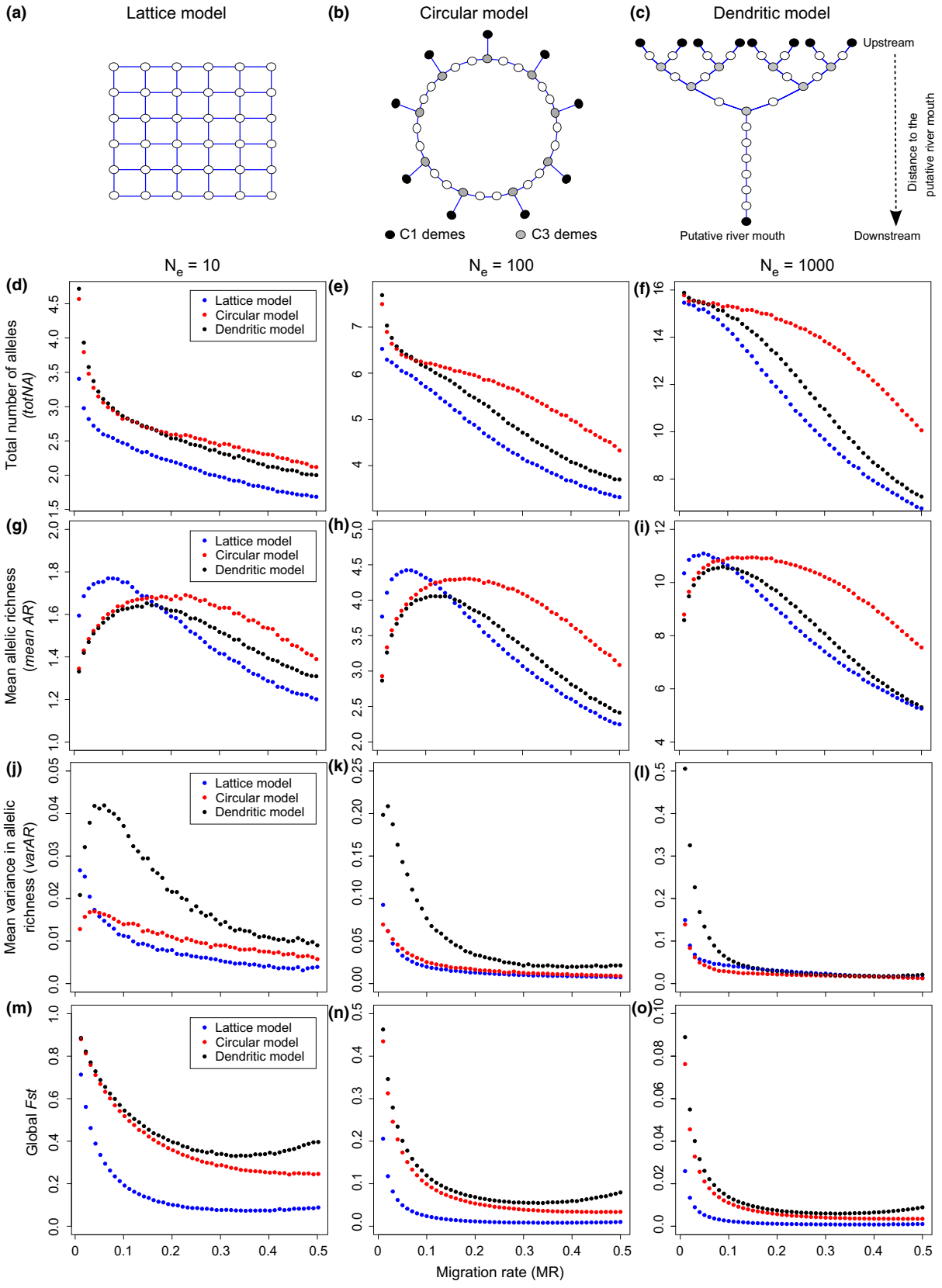
(a)
Lattice model
(b)
Circular model
(c)
Dendritic model
Upstream
Distance to the putative river mouth
C1 demes
C3 demes
Putative river mouth
Downstream
Ne = 10
Ne = 100
Ne = 1000
(d)
(e)
(f)
(g)
(h)
(i)
(j)
(k)
(l)
(m)
(n)
(o)
Lattice model
Circular model
Dendritic model
Total number of alleles (totNA)
Mean allelic richness (mean AR)
Mean variance in allelic richness (varAR)
Global Fst
Migration rate (MR)

Fig. 1 (a) Two-dimensional stepping-stone landscape (lattice model), (b) quasi-circular landscape (circular model) and (c) river network-like dendritic landscape (dendritic model) used to simulate genetic data. Each model was composed of multiple demes (circles) that exchange migrants with their immediate neighbour(s) using dispersal corridors (blue lines). In the circular and dendritic models, we differentiated 'low-connected' demes (C1 demes; black circles) and 'highly connected' demes (C3 demes; grey circles). (d–f) Total number of alleles calculated at the landscape level (totNA), (g–i) mean allelic richness (mean AR) across demes, (j–l) mean variance in allelic richness (varAR) across demes and (m–o) global F_{st} at the landscape level, calculated for each model (blue, red and black dots for the lattice, circular and dendritic models, respectively) in function of the effective deme size (N_e = 10, 100 or 1000) and the migration rate (MR = 0.01 to 0.5).

assessed patterns of isolation by distance (IBD), that is linear relationships between the geographic distance between pairs of demes (in number of demes) and pairwise F_{st} values, as given by the formula $F_{st}/(1–F_{st})$ (Rousset, 1997) for each simulated genetic dataset. We specifically assessed the strength of each linear relationship by calculating Pearson's correlation coefficients (r).

Results

Comparison between lattice, circular and dendritic landscapes

Comparisons between dendritic vs. lattice models revealed that, overall, the total number of alleles (totNA) and global F_{st} values were higher in the dendritic than in the lattice model, irrespective of effective deme sizes (N_e) and migration rates (MR; Fig. 1d–f, m–o). Additionally, varAR was higher in the dendritic than in the lattice model, especially for low-to-intermediate MR values (Fig. 1j–l), suggesting that allelic richness differences among demes were higher in the dendritic than in the lattice model. As predicted, mean AR over demes was lower in the dendritic than in the lattice model, but only for low-to-intermediate MR values (irrespective of N_e); for higher MR values, mean AR was higher in the dendritic than in the lattice model (Fig. 1g–i).

Comparisons between the circular vs. the two other models revealed similarities and differences with both models, depending on the summary statistic being considered. Values of varAR were similar between circular vs. lattice models, especially for N_e of 100 and 1000 (Fig. 1j–l), whereas global F_{st} values observed for circular models were close to those observed for dendritic models (except for high MR values; Fig. 1m–o). Additionally, totNA and mean AR values were similar between circular vs. dendritic models for low MR values, but they were higher in the circular model for intermediate and high MR values, especially for N_e values of 100 and 1000 (Fig. 1d–i).

Comparisons were less straightforward to interpret when totNA, mean AR, varAR and global F_{st} were expressed as a function of the $N_e \times$ MR product. Indeed, values observed for these statistics did not follow single continuous distributions along the $N_e \times$ MR gradient at the landscape level, as they strongly depend upon the assumed N_e *per se* (Fig. S1). Consequently, values of totNA, mean AR and varAR (and to a lesser extent, of global F_{st}) strikingly varied for simulations characterized by identical $N_e \times$ MR but with different N_e values (Fig. S1A–D).

Overall, these results suggest that (i) dendritic connectivity increases β- and γ-genetic diversities and, to a lesser extent, α-diversities in the dendritic landscape, compared to a classical 2D lattice landscape; (ii) these effects are not only due to the connectivity level *per se* of the dendritic landscape, but also to its dendricity; and (iii) the effects of N_e and MR on genetic diversity are difficult to assess by considering the $N_e \times$ MR product as a single explanatory variable.

Comparison between low and highly connected demes in dendritic and circular landscapes

Overall, AR was higher in highly connected demes (C3) than in low-connected demes (C1) for the dendritic model (Fig. 2a). These differences in AR were larger for low N_e (i.e. 10) and decreased as MR increased. Conversely, mean F_{st} values were higher in C1 than in C3 demes (Fig. 2a), with larger differences for low MR (when N_e = 100 or 1000) to intermediate MR values (when N_e = 10; Fig. 2a). Concerning the circular model, AR tended to be higher for C3 demes than that for C1 demes, although differences between deme types were lower than those observed in the dendritic model and were close to zero for large MR (Fig. 2b). Mean F_{st} values were marginally larger for C1 than those for C3 demes for low MR (Fig. 2b), and differences between deme types became highly stochastic when MR values were higher than 0.15.

As for the comparison between the three landscapes, differences in AR and mean F_{st} between C3 and C1 demes did not followed single continuous distributions at the landscape scale when they were expressed as a function of the $N_e \times$ MR product (Fig. S2), hence making the interpretation tricky.

These results show that dendricity, and not only connectivity *per se*, favours allelic richness (AR) in highly connected demes (e.g. confluences in river networks), while favouring genetic differentiation (mean F_{st}) in low-connected demes (e.g. headwaters and river mouths in river networks).

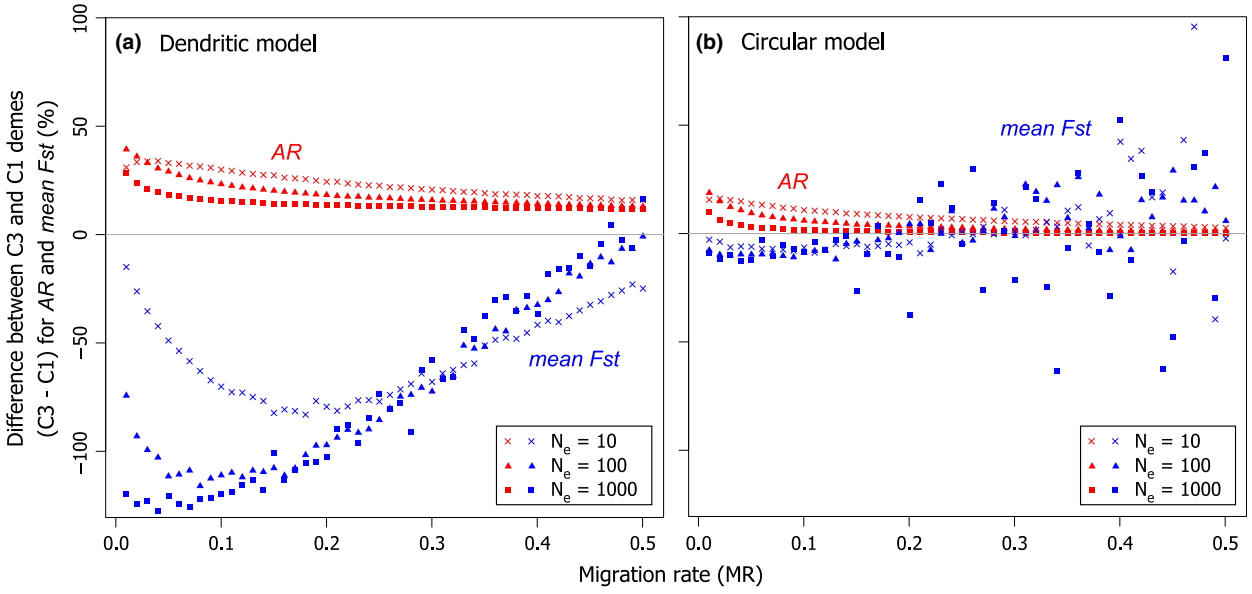

Fig. 2 Differences (expressed as percentages) between C3 demes (i.e. highly connected demes) and C1 demes (i.e. low-connected demes) for allelic richness (AR, red symbols) and for mean genetic differentiation (mean F_{st}, blue symbols) calculated at the deme level for (a) the dendritic model and (b) the circular model. Positive values indicate that C3 demes display higher values than C1 demes, and vice versa. Results are displayed for three values of effective deme size (N_e = 10, 100 and 1000) and increasing values of migration rate (0.01 to 0.5 with 0.01 increments). Several replicates were simulated for each N_e-MR combinations; here, only the average values are shown.

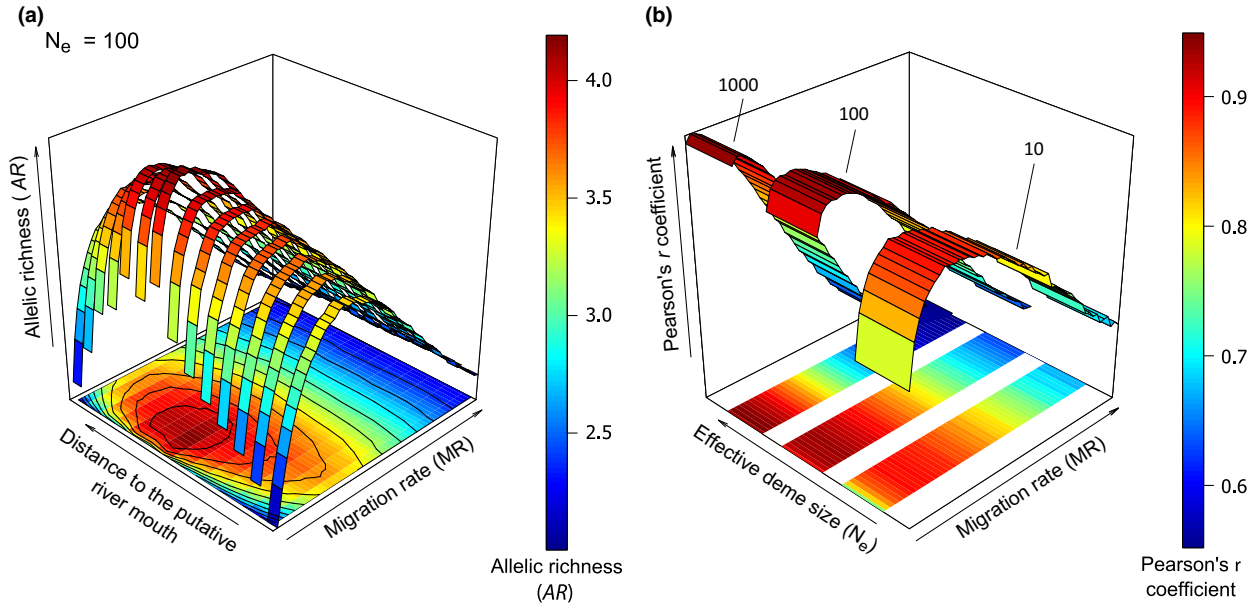

Fig. 3 (a) Perspective plot representing the mean allelic richness calculated over loci per deme (AR, coloured scale) in function of (i) the distance to the putative river mouth of each deme (in number of demes) and (ii) the migration rate (MR) for simulations generated under the dendritic model considering an effective deme size N_e = 100. (b) Perspective plot representing the strength of the isolation-by-distance pattern (measured as the Pearson correlation coefficient r between the distance between pairs of demes (in number of demes) and $F_{st}/(1-F_{st})$ values, coloured scale) in function of (i) the effective deme size (N_e = 10, 100 or 1000) and (ii) the migration rate MR. The coloured surfaces at the square bases are surface projections of the 3D perspective plots.

Spatial patterns of genetic diversity in the dendritic landscape

Regarding the relationships between AR and distance from the putative river mouth in the dendritic model, we detected that for several simulations, AR was higher at demes situated at intermediate distances from the putative river mouth (i.e. in the centre of the network), and lower in the most downstream and upstream demes, hence generating bell-shaped relationships (Fig. 3a for N_e = 100; Fig. S3A,B for N_e = 10 and 1000 respectively). This pattern was particularly strong for low migration rates (i.e. MR between 0.01–0.10) irrespective of N_e, and its strength progressively decreased until reaching a flat relationship as MR increased (Fig. 3a, Figs S3 and S4 for snapshot examples).

Overall, correlations between pairwise F_{st} and distance between demes were strong for all parameter combinations ($r > 0.55$; Fig. 3b). Patterns of IBD were however stronger for intermediate effective deme sizes (N_e = 100) than those for low and high N_e values (10 and 1000; Fig. 3b). For intermediate and high N_e (100 and 1000), the strength of the IBD was strong for low MR values and gradually decreased in strength for intermediate to high MRs, whereas for low N_e (10), the strongest IBD patterns were found at intermediate MR values (Fig. 3b). This shows complex interactions between N_e and MR in shaping IBD in dendritic networks.

Discussion

We showed that dendritic connectivity strongly controlled the level and the distribution of genetic diversity at the meta-population level. We notably demonstrated that, overall, the mean allelic richness over demes was lower in the dendritic than in the lattice landscape (only for low MRs), whereas the total number of alleles observed at the landscape scale, the global F_{st} and variance in allelic richness were higher in the dendritic landscape under most situations. This latter result was probably because in the dendritic landscape, allelic richness was lower in low-connected demes than in highly connected demes, hence generating a strong spatial heterogeneity in allelic richness (which was more reduced in the circular landscape, and absent in the lattice landscape due to its high connectivity level). The difference in allelic richness between low and highly connected demes we highlight here may also explain why, when MRs were low to intermediate, we observed bell-shaped relationships between allelic richness measured at the deme level and the distance of each deme from the river mouth (i.e. increase in allelic richness in the centre of the network). This shows that dendritic connectivity may explain empirical patterns that have been previously observed empirically but remained poorly (or not) explained (Watanabe *et al.*, 2008; Alp *et al.*, 2012).

The increase in allelic richness in highly connected demes (i.e. the nodes situated at the core of the network) in the dendritic landscape may be due to the fact that these demes receive alleles from several demes that are highly genetically differentiated from each other. Accordingly, we demonstrated that mean F_{st} measured at the deme level was strikingly lower in highly connected demes than in low-connected demes in the dendritic landscape for most realistic combinations of effective deme sizes and MRs. Interestingly, the effect of deme connectivity on the spatial distribution of genetic diversity was exacerbated in the dendritic landscape, as differences (both in terms of allelic richness and genetic differentiation) between highly and low-connected demes were much more pronounced in the dendritic and in the circular landscape. To sum up, these results show that dendritic connectivity affects neutral genetic differentiation in dendritic networks, by notably promoting differentiation in the less connected (and hence more isolated) demes (e.g. headwaters). A direct consequence of this dendritic connectivity-driven effect on genetic differentiation is the generation of strong IBD for all combination of effective deme sizes and MRs (which was not the case for the lattice landscape, where the mean Pearson's coefficient calculated across simulations was of 0.451, vs. 0.778 for the dendritic landscape).

The strength of the IBD was, however, strongly dependent upon the interaction between effective deme sizes and MRs: IBD were strong for low MRs when N_e values were intermediate to high, whereas for intermediate MRs, IBD were stronger when N_e was low. These results show that dendritic connectivity, by modulating the degree of intrademic gene flow that is exchanged between demes (i.e. the $N_e \times$ MR product), may deeply influence patterns of IBD in realistic landscapes, hence complementing previous findings from an individual-based theoretical approach (Labonne *et al.*, 2008).

Although it was not a primary goal of the study, our results also show that assessing how genetic diversity evolves as a function of the ongoing level of gene flow occurring between populations can be tricky. Indeed, genetic diversity indices followed continuous distributions when they were expressed in function of MR for given N_e values, but this was not true when they were only expressed as a function of the $N_e \times$ MR product. This was because, contrarily to MRs, there is a direct correlation between effective population sizes and genetic diversity (Frankham, 1996). We therefore recommend the use of multifactorial designs that consider N_e and MR independently in future studies aiming at assessing the effects of effective population sizes and migration on genetic diversity, rather than using the amount of gene flow occurring between populations as a unique explanatory variable.

By adopting a design similar to that of Carrara *et al.* (2012), our results further suggest that dendritic

connectivity similarly shapes biodiversity patterns from meta-community (Carrara *et al.*, 2012) to meta-population levels (this study). Most of the patterns of genetic diversity we highlighted at the meta-population level (e.g. higher variance in allelic richness and F_{st} in the dendritic landscape; lower allelic richness in 'headwater' than in 'confluence' demes) are indeed very comparable to those found by Carrara *et al.* (2012) at the meta-community level. Indeed, Carrara *et al.* (2012) demonstrated that dispersal along dendritic corridors increased species differentiation among local communities (β-diversity) and variance in local species richness (α-diversity; Carrara *et al.*, 2012). In addition, α-diversity was lower in 'headwater communities' (communities situated on the most extreme branches of the network) than in 'confluence communities' (communities situated at the nodes of the network), whereas the opposite pattern was observed for β-diversity (Carrara *et al.*, 2012). This may indicate a general congruency between neutral genetic and species diversity patterns in dendritic networks, which may have both theoretical and conservation implications. For instance, if both genetic and taxonomic diversities are distributed congruently, conservation actions aiming at preserving diversity at one level will benefit the other level. Local characteristics such as habitat availability or heterogeneity have been advocated as major factors underlying co-variation between genetic and species diversity (Vellend & Geber, 2005). Here, we argue that landscape structure *per se* may also generate spatial co-variation in biodiversity metrics. Future empirical studies should be developed to test this hypothesis.

Understanding the overall functioning of dendritic networks is a prerequisite for sustaining biodiversity in these habitats. Here, we focused specifically on connectivity and dendricity, but additional processes such as asymmetric gene flow, colonizations and/or difference in effective deme sizes along environmental and/or geophysical gradients (e.g. the upstream–downstream gradient) have to be conjointly considered for ranking their independent and joint effects on empirically observed biodiversity patterns. Additionally, we focused here on a single specific type of dendritic network assimilated to a river network characterized by high dendricity in the upper/central parts of the network (due to the presence of many tributaries and confluences) and by a linear main stem situated in the downstream part. However, other alternative types of river networks exist (e.g. rectangular or trellis-like networks; see Mejía & Niemann, 2008), and spatial patterns of genetic diversity observed in these networks remain to be explored. We hope that our work will motivate future researches to take into account alternative spatial structures and/or the combined effects of multiple processes and will hence contribute to the development of a general theory on ecological and evolutionary patterns and processes in dendritic habitats.

Acknowledgments

We thank the CALMIP group. This work was performed using HPC resources from CALMIP (allocation P1003). We thank Géraldine Loot, Lounès Chikhi, Julien Cucherousset, Antoine Lecerf, Camille Pagès, Andy Gardner as well as two anonymous referees for insightful comments. Radika Michniewicz corrected the English. This work has been carried out in two research units (EDB & SEEM) that are part of the 'Laboratoire d'Excellence' (LABEX) entitled TULIP (ANR-10-LABX-41). This study is part of the European project 'IMPACT' and has been carried out with financial support from the Commission of the European Communities, specific RTD programme 'IWRM-NET'.

References

Alp, M., Keller, I., Westram, A.M. & Robinson, C.T. 2012. How river structure and biological traits influence gene flow: a population genetic study of two stream invertebrates with differing dispersal abilities. *Freshw. Biol.* **57**: 969–981.

Altermatt, F. 2013. Diversity in riverine metacommunities: a network perspective. *Aquat. Ecol.* **47**: 365–377.

Campbell Grant, E.H., Lowe, W.H. & Fagan, W.F. 2007. Living in the branches: population dynamics and ecological processes in dendritic networks. *Ecol. Lett.* **10**: 165–175.

Carrara, F., Altermatt, F., Rodriguez-Iturbe, I. & Rinaldo, A. 2012. Dendritic connectivity controls biodiversity patterns in experimental metacommunities. *Proc. Natl. Acad. Sci. USA* **109**: 5761–5766.

Chaput-Bardy, A., Fleurant, C., Lemaire, C. & Secondi, J. 2009. Modelling the effect of in-stream and overland dispersal on gene flow in river networks. *Ecol. Model.* **220**: 3589–3598.

Chave, J. 2013. The problem of pattern and scale in ecology: what have we learned in 20 years? *Ecol. Lett.* **16**: 4–16.

Excoffier, L. & Lischer, H.E.L. 2010. ARLEQUIN suite ver 3.5: a new series of programs to perform population genetics analyses under LINUX and WINDOWS. *Mol. Ecol. Resour.* **10**: 564–567.

Finn, D.S., Bonada, N., Múrria, C. & Hughes, J.M. 2011. Small but mighty: headwaters are vital to stream network biodiversity at two levels of organization. *J. North Am. Benthol. Soc.* **30**: 963–980.

Frankham, R. 1996. Relationship of genetic variation to population size in wildlife. *Cons. Biol.* **10**: 1500–1508.

Gotelli, N.J., Anderson, M.J., Arita, H.T., Chao, A., Colwell, R.K., Connolly, S.R. *et al.* 2009. Patterns and causes of species richness: a general simulation model for macroecology. *Ecol. Lett.* **12**: 873–886.

Guisan, A. & Thuiller, W. 2005. Predicting species distribution: offering more than simple habitat models. *Ecol. Lett.* **8**: 993–1009.

Kimura, M. & Weiss, G.H. 1964. The stepping stone model of population structure and the decrease of genetic correlation with distance. *Genetics* **49**: 561–576.

Labonne, J., Ravigne, V., Parisi, B. & Gaucherel, C. 2008. Linking dendritic network structures to population demogenetics: the downside of connectivity. *Oikos* **117**: 1479–1490.

Laval, G. & Excoffier, L. 2004. SIMCOAL 2.0: a program to simulate genomic diversity over large recombining regions in a subdivided population with a complex history. *Bioinformatics* **20**: 2485–2487.

Lawton, J.H. 1996. Patterns in ecology. *Oikos* **75**: 145.

Lischer, H.E.L. & Excoffier, L. 2011. PGDSpider: an automated data conversion tool for connecting population genetics and genomics programs. *Bioinformatics* **28**: 298–299.

Manel, S. & Holderegger, R. 2013. Ten years of landscape genetics. *Trends Ecol. Evol.* **28**: 614–621.

Mejía, A.I. & Niemann, J.D. 2008. Identification and characterization of dendritic, parallel, pinnate, rectangular, and trellis networks based on deviations from planform self-similarity. *J. Geophys. Res.* **113**: F02015.

Morrissey, M.B. & de Kerckhove, D.T. 2009. The maintenance of genetic variation due to asymmetric gene flow in dendritic metapopulations. *Am. Nat.* **174**: 875–889.

Muneepeerakul, R., Bertuzzo, E., Rinaldo, A. & Rodriguez-Iturbe, I. 2008. Patterns of vegetation biodiversity: the roles of dispersal directionality and river network structure. *J. Theor. Biol.* **252**: 221–229.

Múrria, C., Bonada, N., Arnedo, M.A., Prat, N. & Vogler, A.P. 2013. Higher β- and γ-diversity at species and genetic levels in headwaters than in mid-order streams in Hydropsyche (Trichoptera). *Freshw. Biol.* **58**: 2226–2236.

Pauls, S.U., Alp, M., Bálint, M., Bernabò, P., Čiampor, F., Čiamporová-Zaťovičová, Z. *et al.* 2014. Integrating molecular tools into freshwater ecology: developments and opportunities. *Freshw. Biol.* **59**: 1559–1576.

Paz-Vinas, I., Quéméré, E., Chikhi, L., Loot, G. & Blanchet, S. 2013. The demographic history of populations experiencing asymmetric gene flow: combining simulated and empirical data. *Mol. Ecol.* **22**: 3279–3291.

Peterson, E.E., Ver Hoef, J.M., Isaak, D.J., Falke, J.A., Fortin, M.-J., Jordan, C.E. *et al.* 2013. Modelling dendritic ecological networks in space: an integrated network perspective. *Ecol. Lett.* **16**: 707–719.

Pollux, B.J.A., Luteijn, A., Van Groenendael, J.M. & Ouborg, N.J. 2009. Gene flow and genetic structure of the aquatic macrophyte *Sparganium emersum* in a linear unidirectional river. *Freshw. Biol.* **54**: 64–76.

Putman, A.I. & Carbone, I. 2014. Challenges in analysis and interpretation of microsatellite data for population genetic studies. *Ecol. Evol.* **4**: 4399–4428.

Rousset, F. 1997. Genetic differentiation and estimation of gene flow from F-statistics under isolation by distance. *Genetics* **145**: 1219–1228.

Seymour, M. & Altermatt, F. 2014. Active colonization dynamics and diversity patterns are influenced by dendritic network connectivity and species interactions. *Ecol. Evol.* **4**: 1243–1254.

Szpiech, Z.A., Jakobsson, M. & Rosenberg, N.A. 2008. ADZE: a rarefaction approach for counting alleles private to combinations of populations. *Bioinformatics Oxf. Engl.* **24**: 2498–2504.

Vellend, M. & Geber, M.A. 2005. Connections between species diversity and genetic diversity: species diversity and genetic diversity. *Ecol. Lett.* **8**: 767–781.

Watanabe, K., Monaghan, M.T. & Omura, T. 2008. Longitudinal patterns of genetic diversity and larval density of the riverine caddisfly *Hydropsyche orientalis* (Trichoptera). *Aquat. Sci.* **70**: 377–387.

Wegmann, D., Leuenberger, C., Neuenschwander, S. & Excoffier, L. 2010. ABCtoolbox: a versatile toolkit for approximate Bayesian computations. *BMC Bioinformatics* **11**: 116.

Supporting information

Additional Supporting Information may be found in the online version of this article:

Figure S1 (A) total number of alleles calculated at the landscape level (totNA), (B) mean allelic richness (mean AR) across demes, (C) mean variance in allelic richness (varAR) across demes, and (D) global F_{st} at the landscape level, calculated for each model (blue, red and black symbols for the lattice, circular and dendritic models respectively) in function of the ongoing level of gene flow (i.e. $N_e \times$ MR; the number of genes that are transferred between pairs of demes each generation).

Figure S2 Differences (expressed as percentages) between C3 demes (i.e. highly connected demes) and C1 demes (i.e. low-connected demes) for allelic richness (AR, red symbols) and for mean genetic differentiation (mean F_{st}, blue symbols) calculated at the deme level for (A) the dendritic model and (B) the circular model.

Figure S3 Perspective plot representing the mean allelic richness calculated over loci per deme (*AR*, coloured scale) in function of (i) the distance to the putative river mouth of each deme (in number of demes) and (ii) the migration rate (MR), calculated from simulations generated under the dendritic model considering effective deme sizes of $N_e = 10$ (A) and 1000 (B).

Figure S4 Figure representing the mean allelic richness calculated over loci *per* deme (*AR*) in function of the distance to the putative river mouth of each deme (in number of demes) for all combinations of $N_e = \{10; 100; 1000\}$ and MR = {0.02; 0.20; 0.40} for simulations generated under the dendritic model.

Data deposited at Dryad: doi:10.5061/dryad.92tt0

Received 8 August 2014; revised 12 March 2015; accepted 19 March 2015